

Third-order optical nonlinearities of carbon nanotubes in the femtosecond regime

J-S. Lauret, C. Voisin,^{a)} G. Cassabois, J. Tignon, C. Delalande, and Ph. Roussignol
Laboratoire Pierre Aigrain, École Normale Supérieure, 24, rue Lhomond, 75005 Paris, France

O. Jost

Institut für Werkstoffwissenschaft der TU Dresden, D-01062 Dresden, Germany

L. Capes

Laboratoire d'Électronique Moléculaire-CEA/Motorola, 91193 Gif-sur-Yvette, France

(Received 13 April 2004; accepted 30 August 2004)

Femtosecond pump-probe experiments have been carried out on an ensemble of single-wall carbon nanotubes deposited on a glass substrate. Measurements of transient changes of transmission and reflection provide an estimate of the real and imaginary parts of the second-order hyperpolarizability of carbon nanotubes. These values are compared with previous measurements and are discussed in the light of a simple model of the optical nonlinearities near the optical band-gap. © 2004 American Institute of Physics. [DOI: 10.1063/1.1808226]

Single wall carbon nanotubes (SWCNT) have attracted much attention in the last ten years since they exhibit typical behaviors of unidimensional materials especially for electronic and optical properties.^{1,2} The original electronic structure of the nanotubes mainly originates from the sp^2 hybridization of the carbon atoms resulting in a greatly delocalized π -electrons cloud along the tube axis. Theoretical studies show that this configuration leads to a strong enhancement of the nonlinear optical susceptibilities with a fast response time since these nonlinearities mainly result from electronic contributions.³⁻⁵ Since carbon nanotubes also show striking stability under high light flux, they are expected to be a very promising material for new nonlinear optical devices. A few experimental studies have demonstrated the potentialities of carbon nanotubes for third-order harmonic generation, optical Kerr effect or optical limitation in the nanosecond regime.⁶⁻¹⁰ In the femtosecond regime, transient absorption and photoemission measurements on nanotubes either deposited^{11,12} or embedded in a resin¹³ have been interpreted in terms of carrier or exciton dynamics.

In this letter we present an estimation of the electronic contribution to the real and imaginary parts of the third-order susceptibility ($\chi_{xyy}^{(3)}$) of a sample consisting in a 100-nm-thick layer of deposited single wall carbon nanotubes on a glass substrate, and then deduce an estimation of the resonant second-order hyperpolarizability of one nanotube. Indeed the use of femtosecond pulses in the infrared range allows us to probe selectively the resonant electronic contribution to the susceptibility. The imaginary and real parts of the susceptibility are extracted from the transient changes of transmission and reflection in femtosecond pump-probe measurements. This estimation is compared with measurements in other regimes or on other SWCNT-based materials. We also show that a very simple model describing the system as an ensemble of resonantly excited two-level systems is able to reproduce the spectral dependence and order of magnitude of the experimental $\chi^{(3)}$.

^{a)}Electronic mail: christophe.voisin@lpa.ens.fr

The sample consists in single wall carbon nanotubes obtained by laser ablation of a doped graphitic target.¹⁴ The raw material is purified by a usual acid and ultrasonic treatment.¹⁵ The nanotubes are then rinsed out with hydrogenperoxyde and filtered; the residual material, the so-called “bucky paper,” is dispersed through ultrasonic agitation in *N*-Methyl-Pyrrolidone (NMP). This suspension is sprayed on a glass substrate at a temperature of about 200 °C. An atomic force microscope (AFM) inspection of the sample shows a noncontinuous layer of entangled nanotubes and bundles of nanotubes; the typical thickness L of the layer is about 100 nm. The layer is homogeneous on typical size of 1 mm, much larger than the laser spot diameter (about 100 μm).

In bulk proportions, one-third of the SWCNTs are metallic, the others being semiconducting with a gap energy depending on the chirality and roughly proportional to the inverse of the tube diameter.¹⁶ The absorption spectrum of our sample is displayed in the inset of Fig. 1. It consists in a

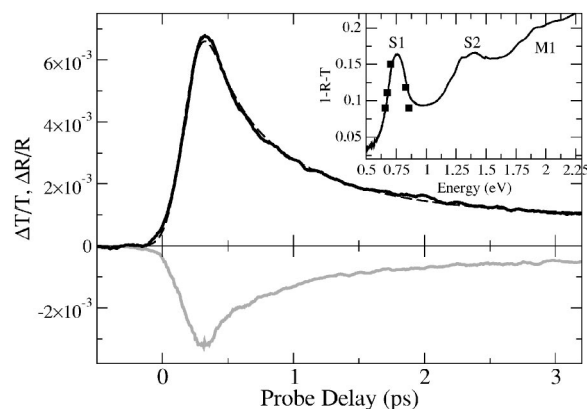


FIG. 1. Transient changes of transmission (black solid line) and reflection (grey line) of a sample of deposited carbon nanotubes in a degenerate cross-polarized pump-probe experiment in resonance with the line S1 (0.75 eV). The dashed line is an exponential fit of the data with $T1=0.8$ ps. Inset: solid line: linear optical absorption spectrum of a sample of deposited single wall carbon nanotubes on a glass substrate; black squares: normalized amplitude of the pump-probe signal at its maximum as a function of the photon energy.

set of lines ranging from 0.7 to 2.2 eV corresponding to the inhomogeneously broadened transitions between the van Hove singularities, hereafter called interband transitions. The two lowest energy lines centered at 0.75 and 1.3 eV (labeled S1 and S2) are attributed to the interband transitions in the semiconducting tubes and the third line (line M1) to the first interband transition in the metallic ones. These absorption spectra are well reproduced assuming a Gaussian distribution of the diameters of the nanotubes with an average diameter of 1.2 nm and a relative width of 10%.² Modeling the layer of nanotubes as an absorbing Fabry–Perot, we have deduced its effective refraction index at 0.7 eV ($n \approx 2.3$) from its reflection and transmission coefficients.

Our pump–probe setup is based on an optical parametric oscillator pumped by a femtosecond mode-locked Ti:sapphire laser. The pulses have a temporal width of about 200 fs and a central energy tunable in the range 0.65–0.85 eV. The energy injection in the nanotubes is achieved by a pump pulse (10 $\mu\text{J}/\text{cm}^2$). The temporal evolution of the pump induced changes of the optical properties is monitored by measuring the reflection and transmission of a weak delayed probe pulse (1 $\mu\text{J}/\text{cm}^2$).

We focus on a degenerate configuration where both the pump and the probe beams have the same wavelength, in resonance with the line S1, i.e., achieving a selective excitation and probing of the semiconducting nanotubes. We observe a transient photobleaching (positive change of transmission) which is directly related to a band filling effect leading to a decrease of the absorption probability at the interband transition energy.^{11,13,17} A simultaneous recording of the probe reflection reveals a decrease of the reflectivity of the sample (negative change of reflection) with however, an amplitude one order of magnitude smaller than the change of transmission (for details see Ref. 11). These observations are interpreted in terms of third-order nonlinear response of the sample ($\chi^{(3)}(\omega, -\omega, \omega)$), i.e., a crossed optical Kerr effect, which is the lowest order nonlinear effect in a layer of randomly oriented nanotubes.

The polarization of the medium at the frequency ω is written in terms of an effective dielectric susceptibility $\underline{P}(\omega) = \epsilon_0 \underline{\chi}^{\text{eff}}(\omega) \cdot \underline{E}(\omega)$, with

$$\underline{\chi}^{\text{eff}}(\omega) = \underline{\chi}^{(1)}(\omega) + 3 \underline{\chi}^{(3)}(\omega, -\omega, \omega) \cdot \underline{e}_p \cdot \underline{e}_p |A_p(\omega)|^2,$$

where \underline{e}_p denotes the unit vector parallel to the electric field of the pump beam and where A_p is its slow varying envelope. This definition of $\underline{\chi}^{\text{eff}}(\omega)$ holds in the frequency domain. However in our case the typical spectral width of the structures in the absorption spectrum are of the order of 200 meV. Thus, in a first approximation, the dispersion of all optical parameters of the material can be neglected on the scale of the laser width (20 meV) and the definition of the effective susceptibility is still valid when introducing the temporal behavior of the field envelop A_p .¹⁸ In our configuration the pump and the probe are cross polarized and the detection polarizer is parallel to the probe direction. Thus in the following χ will denote the $\chi_{xyy}(\omega, -\omega, \omega)$ component of the tensor.

The expression of the transient change of absorption reads: $\Delta\alpha(t) = (3\omega/2nc)\text{Im}[\chi^{(3)}] \cdot |A_p(t)|^2 \otimes R(t)$ where \otimes stands for the convolution product. We assumed a first-order normalized impulsive response $R(t) = H(t)e^{-t/T_1}/T_1$ with a characteristic time T_1 which reflects the population lifetime.

$H(t)$ is the Heaviside function. The real part of the nonlinear susceptibility is related to the change of refraction index of the sample through: $\Delta n = 3 \text{Re}[\chi^{(3)}]/(2n)|A_p(t)|^2 \otimes R(t)$.

From an analysis of the Fabry–Perot effect in the layer, and taking an index of refraction of 1.52 for the BK7 glass substrate, we have deduced:

$$\Delta\alpha L = -1.4 \frac{\Delta T}{T} - 0.3 \frac{\Delta R}{R},$$

$$\Delta n = 1.5 \frac{\Delta T}{T} + 1.1 \frac{\Delta R}{R}.$$

Since $\Delta R/R$ is twice smaller than $\Delta T/T$ in module, the change of absorption is dominated by the relative change of transmission whereas the change of refraction index results from a balance on both changes of reflection and refraction.

Taking a Gaussian shape for the pump pulse, one can fit the experimental changes of transmission and reflection and extract an estimate of the imaginary and real parts of the third-order nonlinear susceptibility. For a decay time T_1 of 1 ps (see Fig. 1), one gets $\text{Im}[\chi^{(3)}] \approx -10^{-16}$ S.I. (-10^{-7} esu) and $\text{Re}[\chi^{(3)}] \approx +10^{-18}$ S.I. (10^{-9} esu). These values are slightly greater than the ones of usual materials for nonlinear optics. For applications, the main drawback of this material is its relatively strong linear absorption (resonant conditions) which however is balanced by a fast time response.

Neglecting the local field correction, we derive an average second-order hyperpolarizability γ for each nanotube of the order of 10^{-29} esu. Assuming a tube length of 1 μm we deduce a contribution $\gamma_C \approx 10^{-35}$ esu per carbon atom. Although the values available in the literature are strongly dispersed (ranging from 10^{-36} esu⁹ to $7 \cdot 10^{-33}$ esu¹⁰), this value is slightly smaller than the ones previously reported in the nanosecond regime (about 10^{-34} or 10^{-33} esu).^{8,10} Indeed in this regime the nonlinearities are larger since they usually include additive slow mechanisms like thermal or reorientation effects. Comparison with other femtosecond measurements is unfortunately impossible since the authors of Refs. 13 and 17 do not provide enough data to deduce any estimation of the intrinsic hyperpolarizability of the nanotubes.

We now compare these experimental values with an estimation resulting from a simple model where the resonantly excited nanotubes are described as a collection of independent two-level systems, neglecting all other optical transitions.³ The polarization P of the medium is deduced from the density matrix formalism. In the relaxation time approximation, γ_1 and γ_2 are the inverse of the population and coherence relaxation times, respectively. For SWCNTs the former is of the order of 4 meV (1 ps) as shown in Fig. 1 whereas estimations for the latter vary from 20 meV (for isolated nanotubes) to 200 meV (estimated from the fit of absorption spectra of bundles of nanotubes).^{19,20} Considering in a first approximation that the pulse duration (about 200 fs) is much longer than the coherence relaxation time (between 20 and 200 fs), we obtain the stationary solution of the Bloch equations:

$$P(\omega) = \int \frac{g(\omega_0) p^2 N / \hbar}{\gamma_2^2 + (\omega_0 - \omega)^2 + 4 \frac{p^2 \gamma_2}{\hbar^2 \gamma_1} |A_p|^2} (\omega_0 - \omega + i \gamma_2) A_p d\omega_0, \quad (1)$$

and eigen frequency of the two-level systems, N is the bulk density of nanotubes. The normalized Gaussian $g(\omega_0)$ denotes the size (and thus frequency) distribution of the nanotubes and reproduces the shape of the inhomogeneous line S1. In the following we use $\delta\omega = \omega - \omega_0$.

Expanding this polarization in powers of the electric field we get the real and imaginary parts of the third-order nonlinear susceptibility:

$$\chi^{(3)} = \int \frac{4g(\omega_0)p^4N\gamma_2}{\hbar^3\epsilon_0\gamma_1(\gamma_2^2 + \delta\omega^2)^2}(\delta\omega - i\gamma_2)d\omega_0. \quad (2)$$

The dipolar momentum p is obtained from the optical density of the layer of nanotubes at the maximum of line S1 and the knowledge of the surface density $N.L$ of nanotubes. We found an order of magnitude of 10^{15} – 10^{16} m⁻² for $N.L$ by two different methods: the first one is based on an AFM inspection of the sample and an estimation of the porosity factor and for the other $N.L$ is deduced from the concentration of the initial suspension of nanotubes. It follows $p \approx 10^{-28}$ S.I.

Then we have deduced a bulk-like value of the imaginary part of $\chi^{(3)}$ of about -10^{-6} esu for a laser wavelength of $1.55 \mu\text{m}$ in resonance with line S1. This value is slightly larger than the experimental value but the discrepancy is not large as compared to the dispersion of the experimental values in the literature. Moreover this estimation strongly depends on the values of parameters which are only approximately known (homogeneous linewidth, thickness and porosity of the layer) and only gives an order of magnitude. However this simple model allows us to connect the linear and nonlinear properties of the nanotubes which are both accessible to the experiment and gives a first estimation of the electronic contribution to the $\chi^{(3)}$. This value corresponds to a contribution of about 10^{-33} per carbon atom which is at least one order of magnitude larger than the one reported for fullerene molecules as expected from theoretical estimations.^{5,10}

The real part of $\chi^{(3)}$ vanishes at exact resonance for an homogeneous line. However in the case of an inhomogeneous line and due to the asymmetrical shape of the density of states in a quasi-one-dimensional material (van Hove singularities), only tubes with a positive detuning can contribute to the nonlinear signal since the others do not absorb light. We thus take a positive detuning of the order of a fraction of the homogeneous width γ_2 . Since $\text{Re}[\chi^{(3)}]/\text{Im}[\chi^{(3)}] = -\delta\omega/\gamma_2$, it follows that the real part of $\chi^{(3)}$ is positive and slightly smaller than the imaginary part, in agreement with the experimental data.

The data displayed in the inset of Fig. 1 show that the magnitude of the Kerr effect is proportional to the absorption of the sample. This is consistent with the inhomogeneous nature of the line since the nonlinear susceptibility of an homogeneous line given by Eq. (2) is in no case proportional

to the absorption. Thus both absorption and $\chi^{(3)}$ dispersion spectra are fully determined by the size distribution of the nanotubes and we end up with the image of several classes of nanotubes contributing independently to the nonlinear response of the sample.

In conclusion we have measured the electronic contribution to the third-order nonlinear coefficients of a layer of single wall carbon nanotubes in resonant conditions. The response time of this nonlinearity, which corresponds to a transient band filling effect, is about 1 ps. We measure high values of nonlinearities that arise from the contribution of mostly one class of nanotubes within the inhomogeneous line. A simple model describing the system as an assembly of independent two-level systems is able to give a qualitative description of the phenomena and the order of magnitude of the nonlinearity.

LPA is “Unité Mixte de Recherche (UMR 8551) de l’ENS, du CNRS et des Universités Paris 6 et 7”. This work was supported by the European grant “SATURN”, Contract No. IST-1999-10593.

- ¹Z. Yao, H. Postma, L. Balents, and C. Dekker, *Nature (London)* **402**, 273 (1999).
- ²X. Liu, T. Pichler, M. Knupfer, M. Golden, J. Fink, H. Kataura, and Y. Achiba, *Phys. Rev. B* **66**, 045411 (2002).
- ³V. Margulis and T. Sizikova, *Physica B* **245**, 173 (1998).
- ⁴G. Slepyan, S. Maksimenko, V. Kalosha, J. Herrmann, E. Campbell, and I. Hertel, *Phys. Rev. A* **60**, R777 (1999).
- ⁵R. H. Xie and J. Jiang, *J. Appl. Phys.* **83**, 3001 (1998).
- ⁶C. Stanciu, R. Ehlich, V. Petrov, O. Steinkellner, J. Herrmann, I. V. Hertel, G. Ya. Slepyan, A. A. Khrutchinski, S. A. Maksimenko, F. Rotermund, E. E. B. Campbell, and F. Rohmund, *Appl. Phys. Lett.* **81**, 4064 (2002).
- ⁷J. Riggs, D. Walker, D. Carroll, and Y. Sun, *J. Phys. Chem. B* **104**, 7071 (2000).
- ⁸S. Botti, R. Ciardi, L. De Dominicis, L. Asilyan, R. Fantoni, and T. Marolo, *Chem. Phys. Lett.* **378**, 117 (2003).
- ⁹X. Liu, J. Si, B. Chang, G. Xu, Q. Yang, Z. Pan, S. Xie, P. Ye, J. Fan, and M. Wan, *Appl. Phys. Lett.* **74**, 164 (1999).
- ¹⁰S. Wang, W. Huang, H. Yang, Q. Gong, Z. Shi, X. Zhou, D. Qiang, and Z. Gu, *Chem. Phys. Lett.* **320**, 411 (2000).
- ¹¹J.-S. Lauret, C. Voisin, G. Cassaboiss, C. Delalande, P. Roussignol, L. Capes, and O. Jost, *Phys. Rev. Lett.* **90**, 057404 (2003).
- ¹²T. Hertel and G. Moos, *Phys. Rev. Lett.* **84**, 5002 (2000).
- ¹³Y.-C. Chen, N. Raravikar, L. Schadler, P. Ajayan, Y. Zhao, T. Lu, G. Wang, and X. Zhang, *Appl. Phys. Lett.* **81**, 975 (2002).
- ¹⁴O. Jost, A. Gorbunov, W. Pompe, T. Pichler, R. Friedlein, M. Knupfer, M. Reibold, H. Bauer, L. Dunsch, M. Golde, and J. Fink, *Appl. Phys. Lett.* **75**, 2217 (1999).
- ¹⁵D. Mawhinney, V. Naumenko, A. Kuznetsova, J. Yates, J. Liu, and R. Smalley, *Chem. Phys. Lett.* **324**, 213 (2000).
- ¹⁶N. Hamada, S. Sawada, and A. Oshiyama, *Phys. Rev. Lett.* **68**, 1579 (1992).
- ¹⁷O. Korovyanko, C. Sheng, Z. Vardeny, A. Dalton, and R. Baughman, *Phys. Rev. Lett.* **92**, 017403 (2004).
- ¹⁸S. Mukamel, *Principles of Nonlinear Spectroscopy* (Oxford University Press, New York, 1995).
- ¹⁹M. F. Lin and K. Shung, *Phys. Rev. B* **50**, R17744 (1994).
- ²⁰J. Lefebvre, Y. Homma, and P. Finnie, *Phys. Rev. Lett.* **90**, 217401 (2003).